

**COATINGS FOR PROTECTION OF EQUIPMENT FOR
BIOCHEMICAL PROCESSING OF GEOTHERMAL
RESIDUES: PROGRESS REPORT FY'97**

Marita L. Allan

November 1997

**Prepared for:
Office of Geothermal Technologies
U.S. Department of Energy
1000 Independence Avenue, S.W.
Washington, DC 20585**

**Energy Efficiency and
Conservation Division**

OFFICIAL FILE COPY

**COATINGS FOR PROTECTION OF EQUIPMENT FOR BIOCHEMICAL
PROCESSING OF GEOTHERMAL RESIDUES: PROGRESS REPORT FY 97**

**M.L. Allan
Brookhaven National Laboratory**

NOVEMBER 1997

**Prepared for:
Office of Geothermal Technologies
U.S. Department of Energy
1000 Independence Ave., S.W.
Washington, D.C. 20585**

**Energy Efficiency and Conservation Division
Department of Applied Science
Brookhaven National Laboratory
Upton, New York 11973-5000**

**This work was performed under the auspices of the U.S. Department of Energy,
Washington, D.C., under Contract No. DE-AC02-76CH000016.**

CONTENTS

	PAGE
SUMMARY.....	iv
1.0 Introduction.....	1
1.1 Corrosion of 316L Stainless Steel.....	1
1.2 Required Coating Properties.....	2
1.3 Selected Coatings.....	3
2.0 Experimental Procedure.....	3
2.1 Specimen Preparation.....	3
2.1.1 316L Stainless Steel.....	3
2.1.2 Thermal Sprayed Coatings.....	3
2.1.3 Spray-and-Bake Fluoropolymers.....	4
2.1.4 Brushable Ceramic-Filled Epoxy.....	4
2.2 Coupon Tests.....	4
2.3 Atlas Cell Tests.....	5
2.4 Cathodic Disbondment Tests.....	6
2.5 Abrasion Tests.....	7
3.0 Results.....	7
3.1 Coupon Tests.....	7
3.2 Atlas Cell Tests.....	7
3.3 Cathodic Disbondment Tests.....	20
3.4 Abrasion Tests.....	21
4.0 Discussion.....	21
5.0 Future Work.....	22
6.0 Conclusions.....	22
7.0 Acknowledgments.....	22
8.0 References.....	23

SUMMARY

Thermal sprayed ethylene methacrylic acid (EMAA) and ethylene tetrafluoroethylene (ETFE), spray-and-bake ETFE and polyvinylidene fluoride (PVDF) and brushable ceramic-epoxy coatings were evaluated for corrosion protection in a biochemical process to treat geothermal residues. The findings are also relevant to other moderate temperature brine environments where corrosion is a problem.

Coupon, Atlas cell, peel strength, cathodic disbondment and abrasion tests were performed in aggressive environments including geothermal sludge, hypersaline brine and sulphur-oxidizing bacteria (*Thiobacillus ferrooxidans*) to determine suitability for protecting storage tanks and reaction vessels. It was found that all of the coatings were resistant to chemical attack and biodegradation at the test temperature of 55°C. The EMAA coatings protected 316L stainless steel from corrosion in coupon tests. However, corrosion of mild steel substrates thermal sprayed with EMAA and ETFE occurred in Atlas cell tests that simulated a lined reactor operating environment and this resulted in decreased adhesive strength. Peel tests to measure residual adhesion revealed that failure mode was dependent on exposure conditions. Long-term tests on the durability of ceramic-epoxy coatings in brine and bacteria are ongoing. Initial indications are that this coating has suitable characteristics. Abrasion tests showed that the ceramic-epoxy had good resistance to the abrasive effects of sludge. Thermal sprayed EMAA coatings also displayed abrasion resistance.

Cathodic disbondment tests in brine at room temperature indicated that EMAA coatings are resistant to disbondment at applied potentials of -780 to -1070 mV SCE for the test conditions and duration. Slight disbondment of one specimen occurred at a potential of -1500 mV SCE. The EMAA may be suited to use in conjunction with cathodic protection although further long-term, higher temperature testing would be needed.

1.0 INTRODUCTION

A biochemical treatment process to detoxify geothermal brines and sludges has been developed at Brookhaven National Laboratory (Premuzic, 1995). Geothermal fluids contain a variety of inorganic elements, heavy metals and radionuclides. These fluids and solids precipitated from the fluids at low temperature are considered hazardous and must be treated before disposal. The biochemical process uses microorganisms to convert toxic metals, including radionuclides, present in geothermal residues into soluble species. The residues can then be disposed in an economic and environmentally acceptable manner. The process also permits recovery of commercially valuable products such as silica for paint fillers, technical grade KCl and precious metals. The untreated residues are corrosive towards ferrous metals due to high chloride content and low pH. Dissolved gases that may be present in brine such as H_2S , NH_3 and CO_2 also contribute to corrosion. The biochemical treatment process typically operates at pH values of 1-2 and temperatures of 50-55°C. Furthermore, the biocatalyst itself is corrosive. Therefore, the corrosivity of both the biocatalyst and residue must be taken into account when selecting materials for processing equipment.

The biochemical process has been demonstrated on a laboratory scale and is now being scaled up. Stainless steel (316L) vessels were available for use in a pilot scale plant. However, coupons of this material underwent corrosion when exposed to the environments of interest and it was necessary to determine suitable protective coatings. In addition, coatings to protect a low cost construction material, such as mild steel, for the planned full scale plant were of interest.

A literature survey was conducted to select potential coating systems and predict the likely performance of 316L stainless steel. Laboratory experiments were then conducted to evaluate coatings and compare the performance of coated steel against 316L. Resistance to attack by geothermal sludges and brines and sulphur-oxidizing bacteria (*Thiobacillus ferrooxidans*) was investigated.

1.1 Corrosion of 316L Stainless Steel

The corrosion behaviour of stainless steels depends on composition. 316L is an austenitic stainless steel with a nominal composition of 2% Mn, 16-18% Cr, 10-14% Ni and 0.03% (max.) C. It differs from Type 316 in that it has a lower carbon content in order to minimize carbide precipitation in the heat affected zone (HAZ) at welds. Corrosion resistance of stainless steels relies on protection imparted by a passive film. 316L stainless steel is susceptible to corrosion, particularly pitting, and stress corrosion cracking in HCl and other high chloride (>1000 ppm) environments due to breakdown of the passive film (e.g., ASM, 1987; Scharfstein, 1977). Corrosion of 316, 316L and other stainless steel in high temperature geothermal fluids has been investigated by others (e.g., Macdonald et al., 1979; Carter and McCawley, 1978; Cramer and Carter, 1980; Needham et al., 1979; Syrett et al.,

1980; Braithwaite and Lichti, 1980). Based on this previous research, Type 316L can be expected to undergo corrosion in geothermal residues with high chloride content.

Microbiologically influenced corrosion (MIC) is reviewed by Borenstein (1994) and Little *et al.* (1992). Sulphur-oxidizing bacteria pose a threat to ferrous metals because they oxidize sulphur or sulphur-bearing compounds to form sulphuric acid. One species of interest for treatment of geothermal residues, *T. ferrooxidans*, is capable of oxidizing ferrous iron in solution to ferric iron, in addition to oxidizing sulphur. *T. thiooxidans* is another sulphur-oxidizing, acid-producing bacteria that has been linked to MIC. Weldments in austenitic stainless steels are also susceptible to MIC (Borenstein, 1993). Most of the literature on MIC of stainless steels refers to sulphate-reducing and iron-oxidizing bacteria. No specific information on corrosion of 316L by *T. ferrooxidans* was found.

1.2 Required Coating Properties

Coatings for protection of the processing equipment from corrosion and abrasion needed to be resistant to chemical attack and biodegradation in the environments and temperature and pH range of interest. The coatings should be easy to apply as a continuous film to vessels, economic, low VOC, not require priming or post curing, and retain adhesion and protective behaviour throughout the design life of the equipment. Permeation of aggressive species through the coating should be prevented or minimized and the coating should withstand any corrosion products that may develop at the substrate. The use of elevated temperatures in the biochemical process and the interest for coatings in other geothermal environments requires consideration of thermal mismatch. Hence, the coatings should be able to withstand stresses induced at the interface due to different coefficients of thermal expansion between the coating and the substrate. Polymer or polymer-ceramic composite coatings were selected for investigation due to their wide use in the chemical processing industry and properties compatible with service requirements.

Polymers potentially meeting these requirements included epoxies, polyesters and vinyl esters (all with inorganic fillers), an ethylene methacrylic acid copolymer and fluoropolymers. Application methods for fluoropolymers include spray-and-bake and sheet linings. Examples of the latter for transport of corrosive chemicals are provided by Heffner (1992). The spray-and-bake method requires appropriately sized ovens and large pieces of equipment can only be applied at limited facilities. However, this application method may be of interest in geothermal environments for suitably sized workpieces. Sheet linings have a backing which can be used with an elastomeric adhesive.

The application methods selected for investigation were spraying, spray-and-bake and painting. Spraying included thermal spraying in which the polymer powder is melted and impacted against the preheated substrate where it solidifies. This is a 100% solids method that can be used in the field. Case histories of thermal sprayed ethylene methacrylic acid (EMAA) are provided by Loustannau and Horton (1994) and these include rail cars and

wastewater clarifiers. EMAA can also be applied by conventional fluidized bed and electrostatic methods. The other form of spraying considered was conventional application of a liquid coating.

1.3 Selected Coatings

The coatings selected for initial evaluation were: thermal sprayed ethylene tetrafluoroethylene (ETFE) and ethylene methacrylic acid (EMAA) polymers; spray-and-bake ETFE and polyvinylidene fluoride (PVDF) and a brushable ceramic-epoxy. Other coatings may have potential for the application of interest. However, the long-term nature of the evaluations restricted the number of coatings that have been tested to date.

2.0 EXPERIMENTAL PROCEDURE

2.1 Specimen Preparation

2.1.1 316L Stainless Steel

Bare 316L coupons (25.4 x 50.8 x 3.2 mm) were abraded with 120 silicon carbide paper to provide a uniform surface. In order to determine the corrosion resistance of welds, autogeneously welded 316L coupons were also tested. The coupons were supplied by Metal Samples (AL) and had a 120 grit finish. The dimensions of the welded coupons were 19.0 x 50.8 x 3.2 mm.

2.1.2 Thermal Sprayed Coatings

The EMAA copolymer powder was supplied by PFS Thermoplastic Powder Coatings (PF 111). A PFS 124 Powder Pistol with fluidized powder feed was used to apply the EMAA coatings. The propane and compressed air pressures were 41 and 826 kPa, respectively. The standoff distance used for coating test panels was 30-40 cm and the traverse rate was 10 cm/sec. The flow rates of the fluidized bed, combustion air, powder carrier air and propane were 20-25 l/min, 20 l/min, 50 l/min and 8 l/min, respectively. After blasting with alumina grit the panels were preheated to 82°C and then sprayed.

The ETFE powder was supplied by DuPont. The powder was sprayed using a Eutectic + Castolin Terodyn 3000 gun with TecFlow 5102 Powder Feeder. An air shroud at 241 kPa was used. Oxygen, acetylene and nitrogen pressures were 207, 103 and 344 kPa, respectively. The standoff distance was 15 cm and the traverse rate was 10 cm/sec. The grit blasted substrates were preheated to 162°C before spraying. All thermal spraying in this project was conducted at the Thermal Spray Laboratory, Department of Materials Science and Engineering, State University of New York at Stony Brook.

2.1.3 Spray-and-Bake Fluoropolymers

Mild steel coupons coated with PVDF and ETFE were supplied by General Plastics (NJ) for testing. The substrates were sandblasted, preheated and sprayed with fluoropolymer. The coupons were then baked in an oven to fuse the coating. The thickness of the PVDF coating was $1047 \pm 26 \mu\text{m}$. The ETFE coatings had a thickness of $900 \pm 32 \mu\text{m}$.

2.1.4 Brushable Ceramic-Filled Epoxy

The brushable ceramic-filled epoxy coating was supplied by ITW Devcon. Parts A and B were mixed at the recommended proportion and the coating was brush applied to alumina grit blasted mild steel panels. The thickness of the coatings was $1072 \pm 180 \mu\text{m}$. The application method resulted in a relatively high variation in coating thickness.

2.2 Coupon Tests

316L stainless steel coupons coated with EMAA and mild steel coupons with baked PVDF and ETFE were exposed to untreated geothermal sludge, brine residue from the Geysers with $\text{pH} = 2.6$, synthetic hypersaline brine, and *Thiobacillus ferrooxidans* in an experimental set up conforming to ASTM G 31. The EMAA coating thickness was approximately $700 \mu\text{m}$. Bare plain and welded coupons were also tested for comparison. Coupons were suspended in a heated glass flask to give exposure conditions corresponding to complete immersion, partial immersion and vapour zone. Three coupons per exposure condition were tested for all of the environments. The bare 316L coupons were cleaned in a HNO_3 solution at 60°C in accordance with ASTM G1-C7.1.

The untreated geothermal sludge had a water content of 40% by mass. In the dry state the sludge largely consisted of silica (62%), $\text{Fe}_3\text{O}_4 + \text{FeSiO}_4$ (15%), $\text{BaSO}_4 + \text{BaCl}_2$ (4%) and $\text{CaSO}_4 + \text{CaCO}_3$ (3%). The minor components included 6000 ppm NaCl, 1300 ppm KCl, 6000 ppm SrSO_4 , 3500 ppm MnSO_4 , 300 ppm $\text{AsS}_2 + \text{FeAs}_2$, 250 ppm CuS and 130 ppm ZnS. The pH of the wet sludge was 6.12 and the test temperature was 55°C . The sludge was mechanically stirred and aerated throughout the test.

The synthetic brine consisted of 58,000 ppm NaCl, 25,000 ppm CaCl_2 , 15,000 ppm KCl, 1000 ppm FeCl_2 , 930 ppm MnCl_2 , 430 ppm SrCl_2 , 410 ppm LiCl, 370 ppm ZnCl_2 , 330 ppm H_3BO_3 and 130 ppm BaCl_2 . The pH of the brine was 4.15. The brine was aerated throughout the test.

The nutrient for the *T. ferrooxidans* bacteria was prepared from two parts. Part A consisted of 0.4 g $(\text{NH}_4)_2\text{SO}_4$, 0.2 g KH_2PO_4 , 0.08 g $\text{MgSO}_4 \cdot 7\text{H}_2\text{O}$ and 400 ml distilled water. Part B consisted of 22.11 g $\text{FeSO}_4 \cdot 7\text{H}_2\text{O}$, 1.0 ml 1N H_2SO_4 and 100 ml distilled water. Parts A and B were autoclaved separately and then combined aseptically. This was then inoculated with *T. ferrooxidans*. The pH of the *T. ferrooxidans* medium at the start of the test was 2.28

and decreased to 1.98 throughout the course of the test. The temperature of the *T. ferrooxidans* medium was maintained at 55°C and the medium was changed every four weeks. Air was bubbled into the medium. For all environments the test duration was 12 weeks.

2.3 Atlas Cell Tests

The chemical resistance and corrosion protective nature of the coatings under simulated service conditions were determined following the test method described in ASTM C 868 (Atlas Cell Test). In this experimental arrangement coated panels were exposed to immersion and vapour zones, in addition to a temperature gradient from the external bare surface to the internal coated surface. This gradient simulated that which an internally heated reactor vessel would generate and is of importance since a temperature differential can accelerate permeation of the coating.

The test cell basically consisted of a horizontally-oriented, open-ended glass cylinder with a diameter of 152 mm to which the coated panels were clamped on the ends. Neoprene gaskets were placed between the glass and panel to provide a seal. The glass cylinder had ports for a thermometer, immersion heater, air bubbler and reflux condenser. The cylinder was partially filled with 1.2 l of the solution of interest.

The test solutions were synthetic hypersaline geothermal brine (same composition as above) and *T. ferrooxidans* medium. The starting and final pH values of the *T. ferrooxidans* were approximately the same as those for the coupon tests and the medium was changed every four weeks. Air was bubbled into the test cells to provide agitation.

Mild steel panels, 191 x 191 x 6.3 mm (or 204 x 204 x 6.3 mm), were grit blasted and coated with either EMAA, ETFE or Devcon Brushable Ceramic. The thickness of the EMAA coating exposed to brine was 1782 ± 143 μm . The ETFE coating thickness was 463 ± 61 μm . The thickness of the EMAA coatings for the *T. ferrooxidans* test was 768 ± 106 μm . The test temperature was 55°C and the duration was 18 weeks in all cases. The temperature of the external bare steel surface was 43.3-43.9°C.

At the completion of the tests the coated panels were visually examined for signs of deterioration such as blistering, discolouration and loss of gloss. The residual adhesion was determined for EMAA coatings by measuring the peel strength (ASTM D 3167). The plates were cut into strips 25 mm wide and the orientation was vertical so that the strip traversed the vapour and immersion-exposed zones. The strips cut from the outer edges of the plates were beyond the exposure zone. A schematic diagram of the strips cut from the panels is presented in Figure 1. The coatings were peeled back approximately 40 mm using a razor blade to enable the coating to be gripped. An Instron tensile testing machine was used. The crosshead speed was 152 mm/min. It was not possible to measure the peel strength of the ETFE coatings because the material was too brittle to bend 90°.

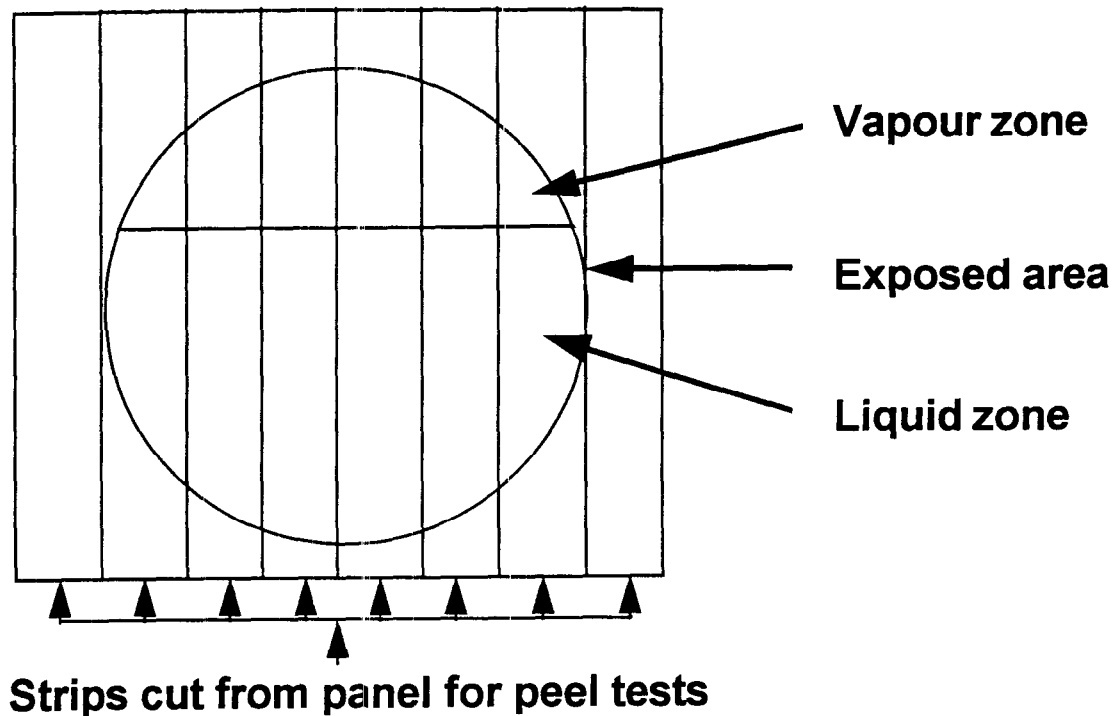


Figure 1. Schematic diagram of peel test specimens cut from Atlas cell panels.

2.4 Cathodic Disbondment Tests

The resistance of EMAA coatings to cathodic disbondment when exposed to an impressed current and hypersaline brine was determined. The objective was to determine whether disbondment around a coating defect would occur under cathodic protection. ASTM G 95 (Attached Cell Method) was used, although the specimen dimensions differed. Mild steel panels 104 x 104 x 4.7 mm were grit blasted and sprayed with EMAA. The average coating thickness was $1090 \pm 110 \mu\text{m}$. A holiday (defect) of 3.2 mm diameter was created by drilling through the coating in the centre of the panel. A glass tube 76 mm diameter was attached to the coated panel with a silicone sealant. The tube was filled with brine and a Pt wire was used as an anode.

Four test potentials were used to reflect different levels of cathodic protection. These were -780, -900, -1070 and -1500 mV SCE. Potentials were monitored daily and adjusted as necessary. Tests were conducted on triplicate coated panels. In addition, control tests in which no cathodic protection current was applied were performed. The duration of the cathodic disbondment tests was four weeks and all tests were conducted at room temperature. At the completion of the tests the diameter of the holiday was measured and the surrounding coating inspected for disbondment. Future tests may examine the effect of temperature on disbondment.

2.5 Abrasion Tests

A small scale test was performed to simulate the abrasion conditions to which a lined vessel containing continuously stirred geothermal sludge would be subjected. A 7.6 l stainless steel tank with a diameter of 203 mm was grit blasted and coated on the internal surface with EMAA. The coating thickness was approximately 700 μm . The tank was half filled with sludge and stirred using a Jiffy mixer blade. Tests were conducted at room temperature and proceeded for two weeks. The coating was visually inspected for wear and the weight loss determined.

3.0 RESULTS

3.1 Coupon Tests

The uncoated 316L coupons tested in untreated geothermal sludge underwent slight general corrosion when partially immersed or exposed to the vapour zone. The EMAA coated coupons did not exhibit any signs of deterioration. The bare 316L coupons totally immersed in synthetic brine showed pitting corrosion with pit depths up to 1200 μm . Crevice corrosion also occurred underneath the PTFE spacer washers between coupons. The partially immersed coupons exhibited pitting corrosion just above the liquid level. Pits up to 1000 μm deep were evident. No visible corrosion was observed for the bare coupons in the vapour zone of the synthetic brine.

Bare 316L coupons exposed to the brine residue from The Geysers exhibited pitting and crevice corrosion when immersed or partially immersed. Evaporation caused salts to form at the liquid/vapour interface and corrosion was severe under these deposits, with pits up to 2000 μm . The coupons in the vapour zone displayed slight surface corrosion. Welded coupons did not undergo preferential corrosion in the brines. 316L coupons coated with EMAA were unattacked by the brines. The baked PVDF and ETFE coatings also withstood the brine environments.

The tests in *T. ferrooxidans* showed that bare 316L was susceptible to general corrosion in the vapour zone. The immersed bare coupons exhibited biofouling, although no corrosion was evident underneath the biofilm. No preferential corrosion in the HAZ of the welded coupons was observed. The EMAA coatings exposed to *T. ferrooxidans* did not show any visible signs of deterioration. Biofouling also occurred to a lesser degree on the immersed coated coupons. The biofilm was less adherent to the EMAA than the bare 316L. The baked ETFE and PVDF coatings were unaffected by the bacteria, although biofouling did occur.

3.2 Atlas Cell Tests

Figures 2 and 3 show the surfaces of the coated panels after testing. Staining due to

evaporation of iron salts is evident at the transition between the liquid and vapour zones. One of the ETFE coated panels tested in brine exhibited eight blisters 5-10 mm in diameter below the liquid level and three blisters of the same diameter at the liquid/vapour interface. The blisters contained fluid and the coating was poorly bonded in the surrounding area. The coating could be peeled by hand as far as the gasket line. Where the coating was not exposed (outside the gasket), adhesion was sound. Corrosion had occurred where the coating was blistered. Spotty black corrosion products (probably Fe_3O_4) existed under the coating in the vapour zone. The spots were typically 2-5 mm in diameter. The coating was not blistered in these areas, but adhesion was decreased. The companion ETFE exposed to the same solution had one blister 5 mm in diameter below the liquid level and corrosion in the vapour zone. The black corrosion products tended to convert to red after exposure to air. The ETFE itself did not undergo any degradation.



Figure 2. Surface of EMAA panel exposed to brine.

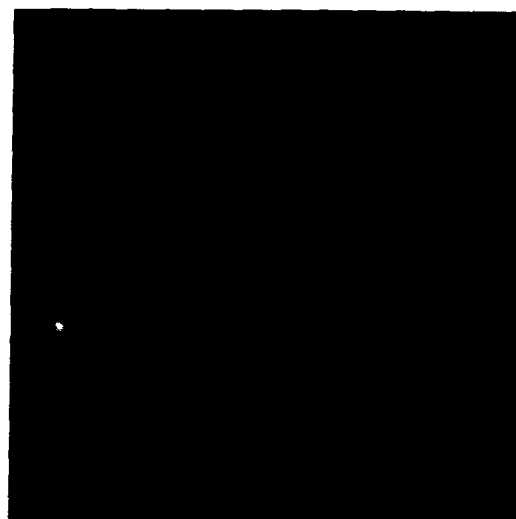


Figure 3. Surface of ETFE panel exposed to brine.

The EMAA coated panels exposed to brine did not exhibit any visible signs of deterioration. As shown in Figure 2, slight surface staining occurred, particularly in a 5-10 mm band at the liquid/vapour zone interface and this was attributed to evaporation of iron salts from the brine. Peel tests revealed black corrosion products beneath the coatings. In one panel, corrosion was more prevalent in the vapour zone, whereas the other exhibited corrosion in both the vapour and liquid zones. For the latter panel, the spots of corrosion in the upper half of the liquid zone were larger in diameter (4-9 mm) than those in the lower half and the vapour zone (0.5-4 mm). The spots of corrosion were randomly distributed. The failure load and mode were dependent on the presence of corrosion products. Failure was predominantly adhesive, although localized areas of cohesive failure within the polymer also occurred, particularly where the surface was free from corrosion. Mixed adhesive/cohesive failure was observed in a 5-10 mm band above the liquid level where the extent of corrosion was less than for other areas in the vapour zone. This band above the liquid level

corresponded with the film of iron salts deposited on the coating external surface. It is proposed that the film acts as a sealant for the coating. Cohesive failure was also evident where the gasket contacted the coating. Corrosion products adhered to both the steel and polymer fracture surfaces.

Figure 4 depicts the peel load versus displacement curve for a strip cut from the edge of one of the panels. The coating in this location was not exposed to brine. The peel force was relatively constant and the failure mode was adhesive. The average peel strength was 4.33 N/mm. The steel and polymer surfaces after peeling are shown in Figure 5. Figure 6 shows the results for a strip cut through an exposed area. The peel force was low in the initial region and this corresponded to the presence of corrosion products at the interface. The increase in peel force at higher displacement occurred outside the exposed area (at the gasket and beyond). Peel strength varied from 1.97 to 6.97 N/mm. Figure 7 shows the peeled steel and polymer surfaces. Figure 8 is another example of low peel forces in the corroded exposed area and increased values before and after this. Plastic deformation of the coatings occurred during peeling and this was concentrated in the areas outside the test cell where greater force was required to remove the coating. Figure 9 shows the peeled steel and polymer surfaces corresponding to the force-displacement curve in Figure 8. All of the above tests were taken from the EMAA panel with corrosion in both the liquid and vapour zones.

The following peel test descriptions are for the panel exposed to brine with corrosion predominantly in the vapour zone. Figures 10 and 11 present typical peel test results for specimens cut through the exposed zone. Both of these figures show great variation in peel force along the length of the specimen. Low peel forces corresponded with the presence of oxides at the interface and adhesive failure. Increased forces in the exposed area correlated with cohesive or mixed adhesive/cohesive failure. Force required to peel the coating typically increased towards the end of the specimens beyond the test cell. In these specimens the peel strength varied from 0.98 to 10.87 N/mm. The surfaces of two of the specimens after peeling are shown in Figures 12 and 13. Cohesive failure of the polymer is evident, as are oxides predominantly in the vapour zone. The peel test result for a strip cut through the edge of the exposed zone is shown in Figure 14. Cohesive failure occurred beneath where the gasket contacted the polymer coating and peel strength ranged from 5.51 to 11.02 N/mm. Figure 15 shows the more constant force required to peel the coating outside the exposed zone. The average peel strength is around 5.51 N/mm.

Fracture surfaces from the EMAA-mild steel peel tests were examined under a scanning electron microscope (SEM). An example of mixed adhesive/cohesive failure in an uncorroded area is shown in Figure 16. The dark areas are polymer adhering to the steel surface. Spherical pores, 100 - 200 μm diameter, in the polymer are evident and failure often occurred through these pores. Figure 17 is a higher magnification view of a fractured pore. Figure 18 shows the steel surface at the liquid/vapour transition zone. Spots of corrosion product are indicated. The polymer adhered to the steel in the uncorroded areas. Where corrosion occurred, failure was between the polymer and corrosion products, or within the

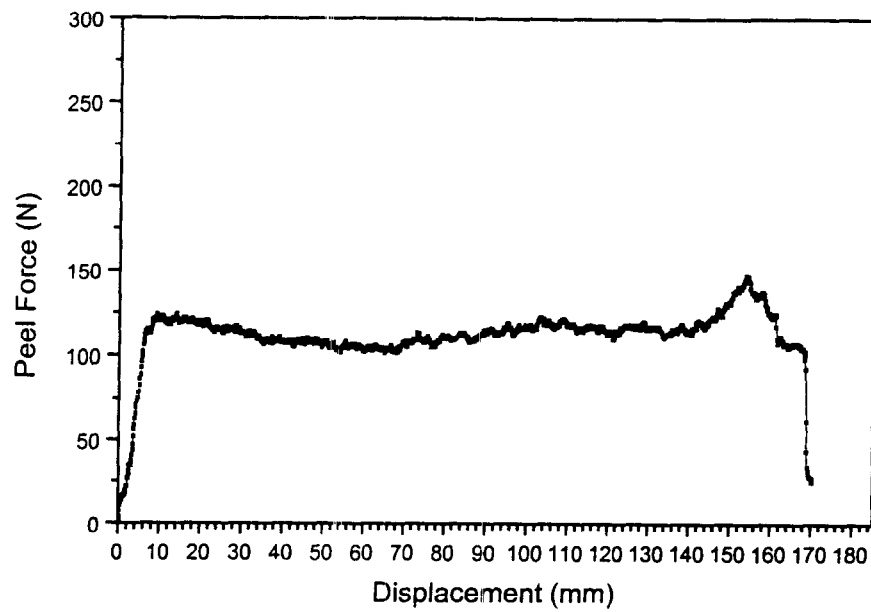


Figure 4. Peel force-displacement curve for EMAA outside brine-exposed zone.

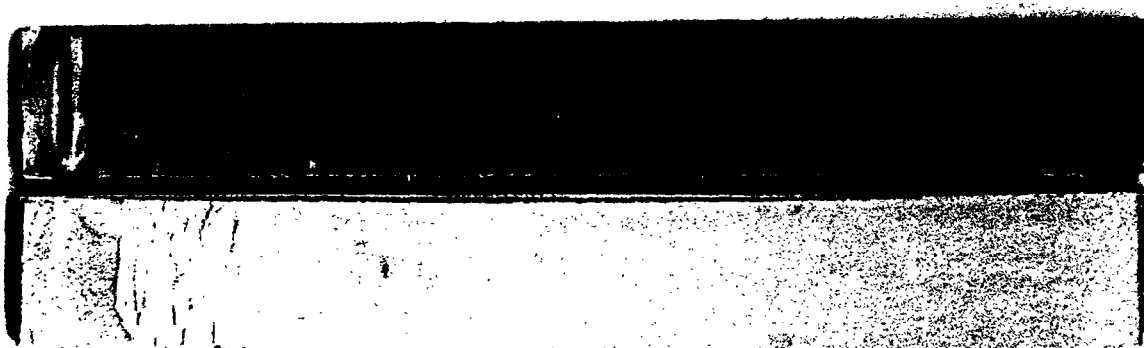


Figure 5. Steel and polymer fracture surfaces corresponding to Figure 4.

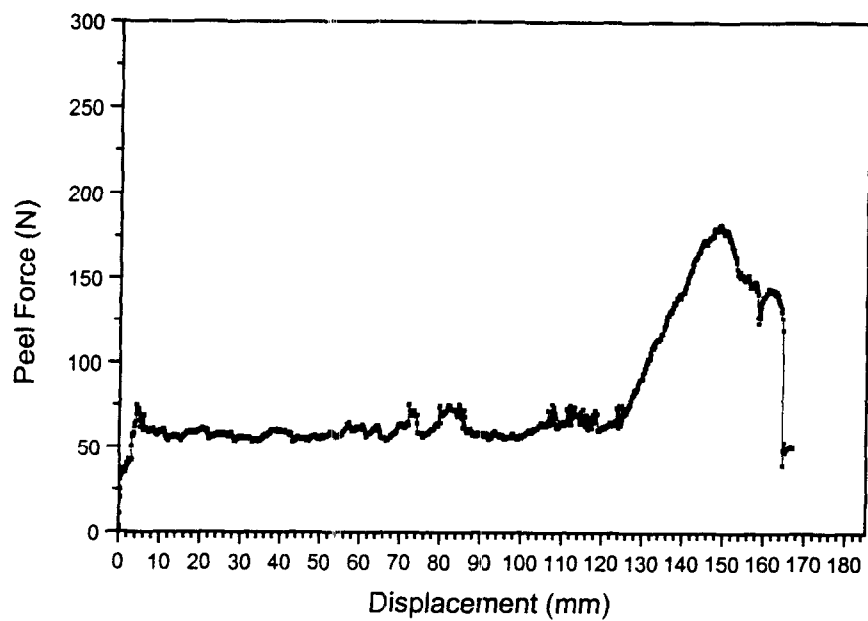


Figure 6. Peel force-displacement curve for EMAA exposed to brine.



Figure 7. Steel and polymer fracture surfaces corresponding to Figure 6.

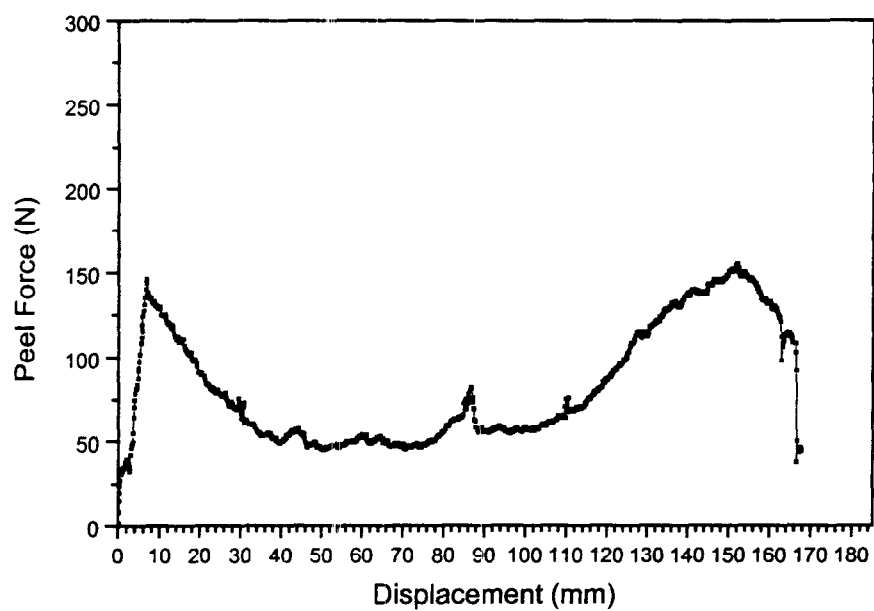


Figure 8. Peel force-displacement curve for EMAA exposed to brine.

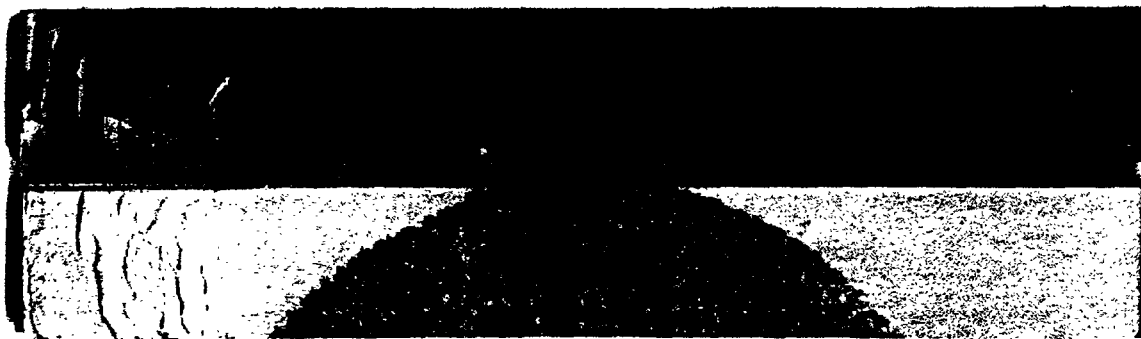


Figure 9. Steel and polymer fracture surfaces corresponding to Figure 8.

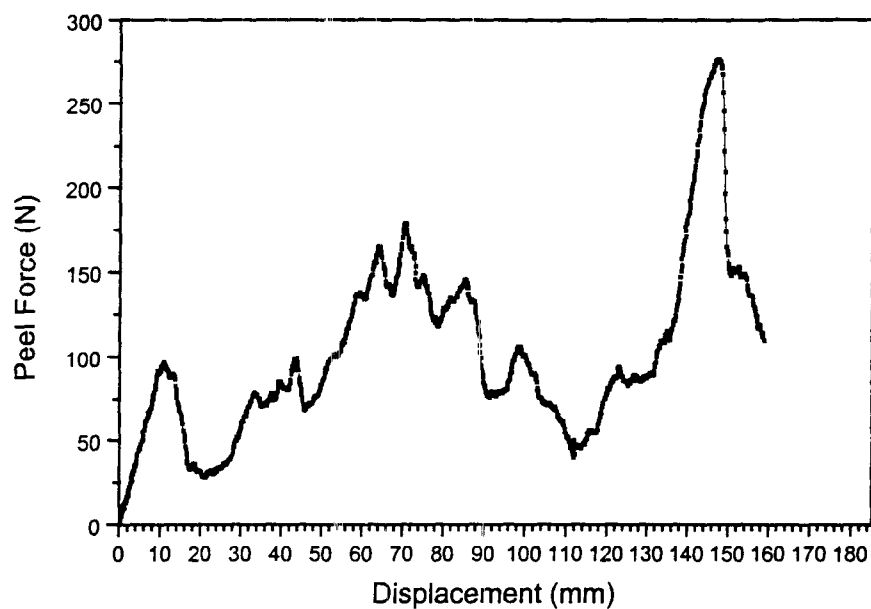


Figure 10. Peel force-displacement curve for EMAA exposed to brine.

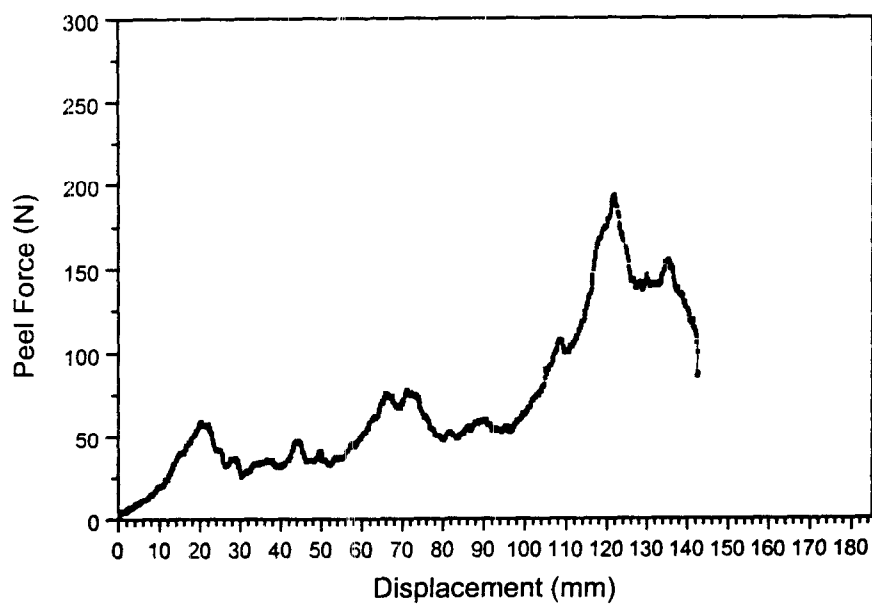


Figure 11. Peel force-displacement curve for EMAA exposed to brine.

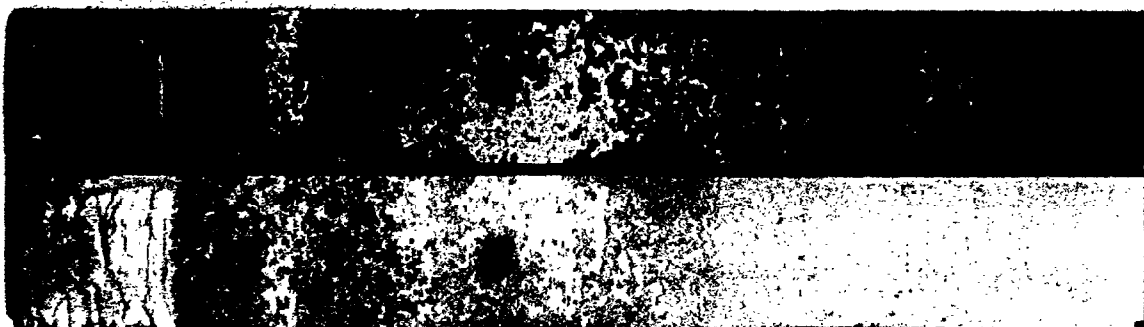


Figure 12. Steel and polymer fracture surfaces for EMAA exposed to brine.

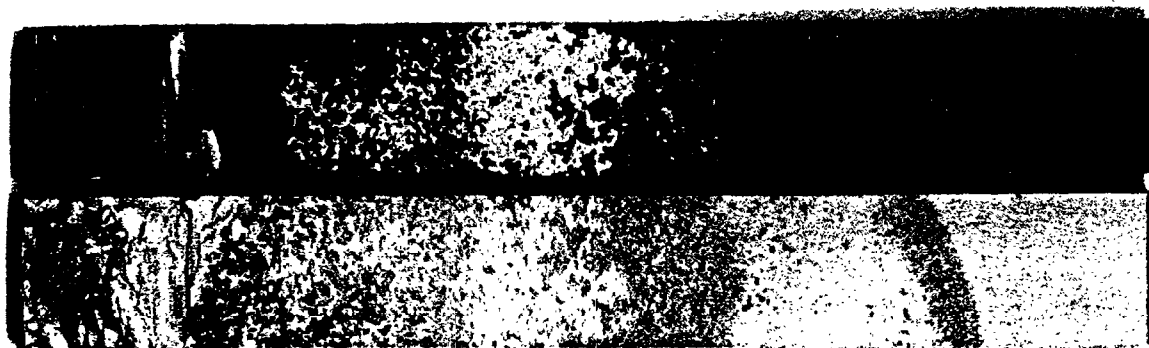


Figure 13. Steel and polymer fracture surfaces for EMAA exposed to brine.

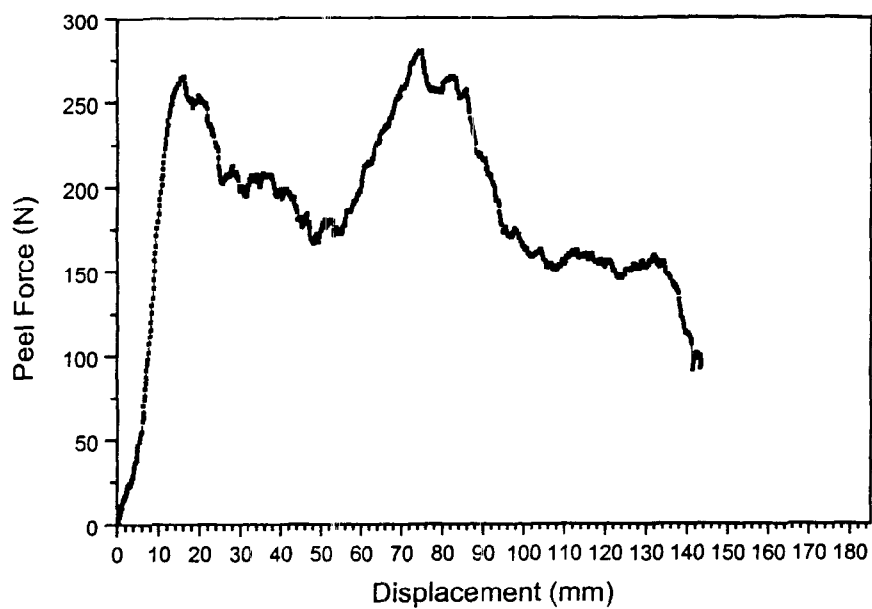


Figure 14. Peel force-displacement curve for EMAA at edge of brine-exposed zone.

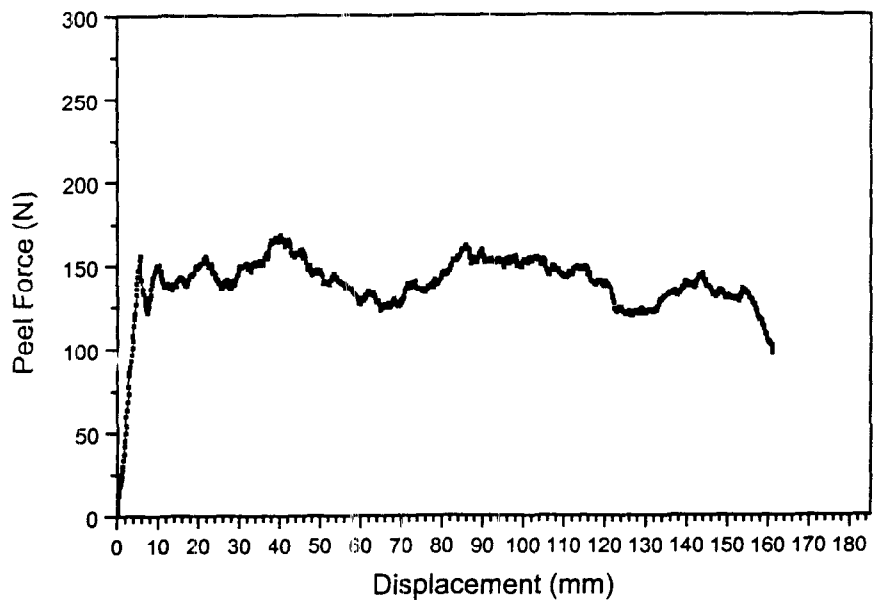


Figure 15. Peel force-displacement curve for EMAA outside brine-exposed zone.

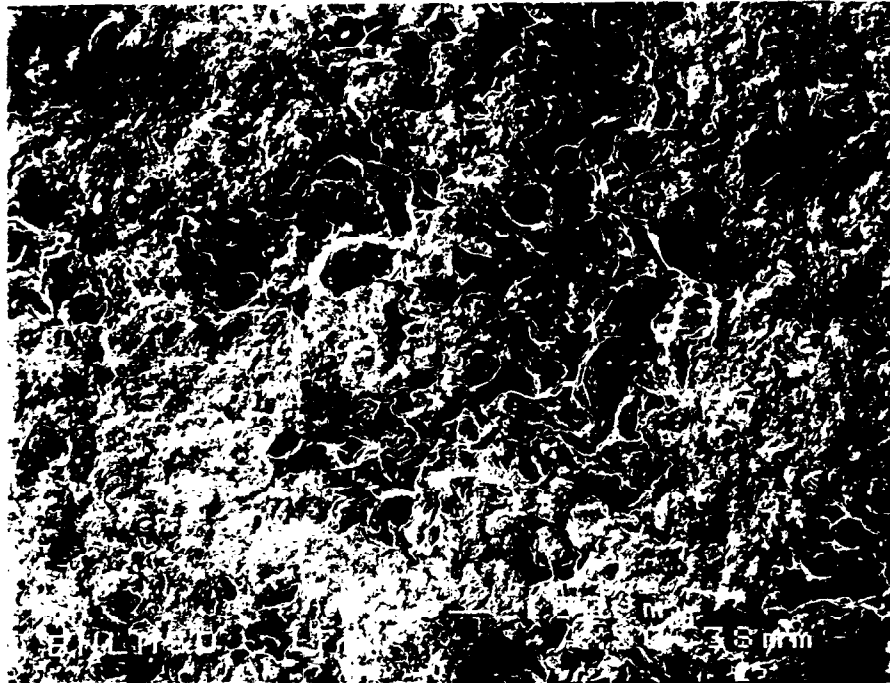


Figure 16. SEM micrograph of steel fracture surface showing mixed adhesive/cohesive failure. Dark areas are polymer.

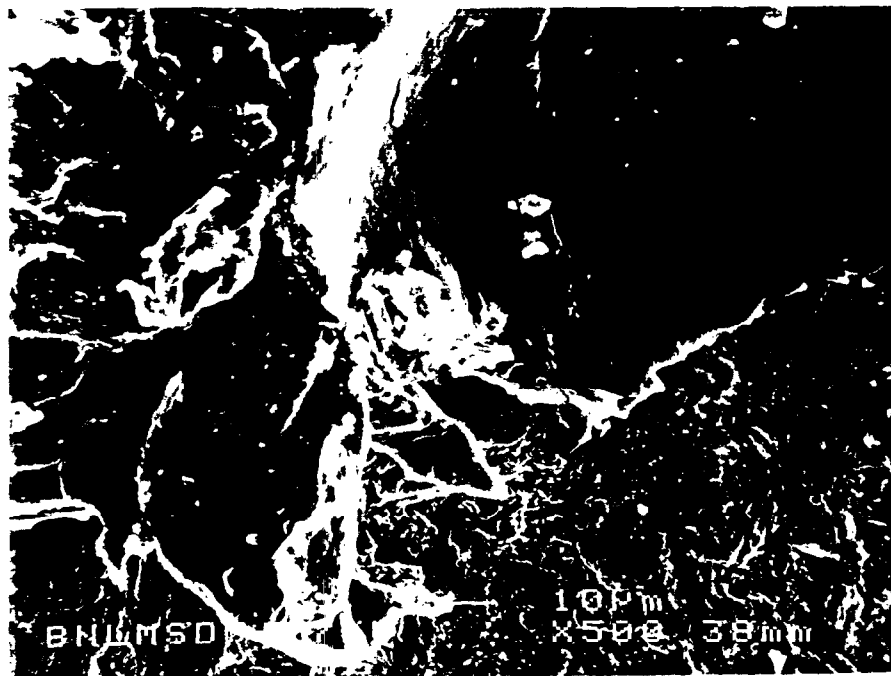


Figure 17 Higher magnification view on Fig. 16 showing failure through pore in polymer.



Figure 18. SEM micrograph of steel fracture surface. Dark areas are polymer, light areas are iron oxides (arrowed).

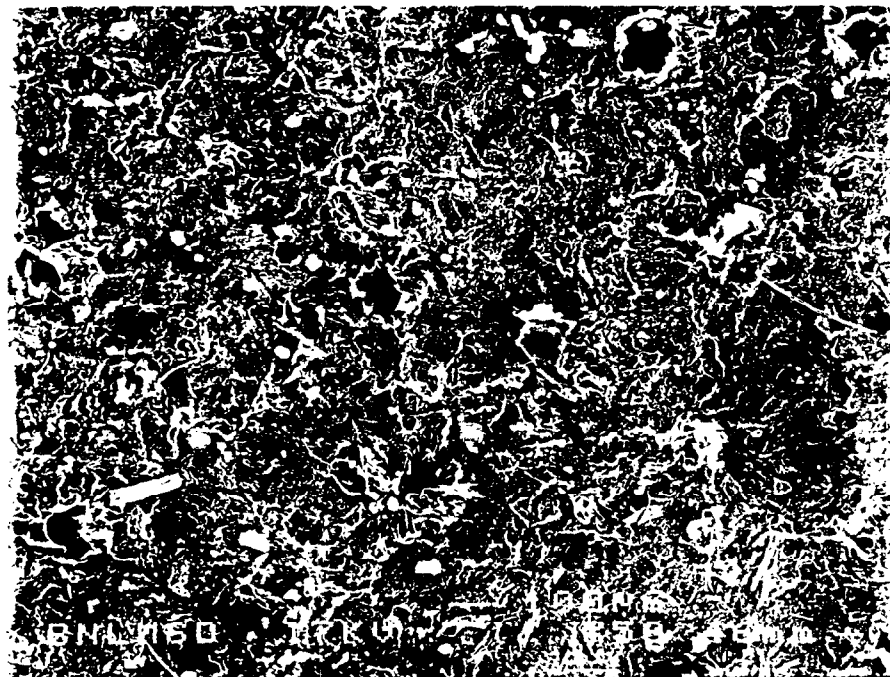


Figure 19 SEM micrograph of polymer fracture surface showing pores.

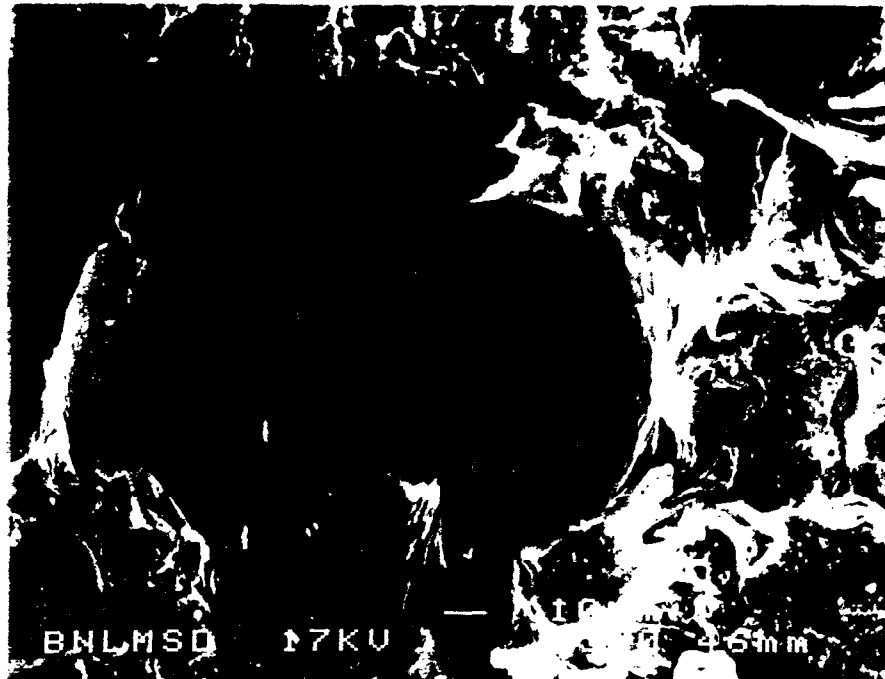


Figure 20 Polymer fracture surface at higher magnification showing ductile tearing around edge of pore

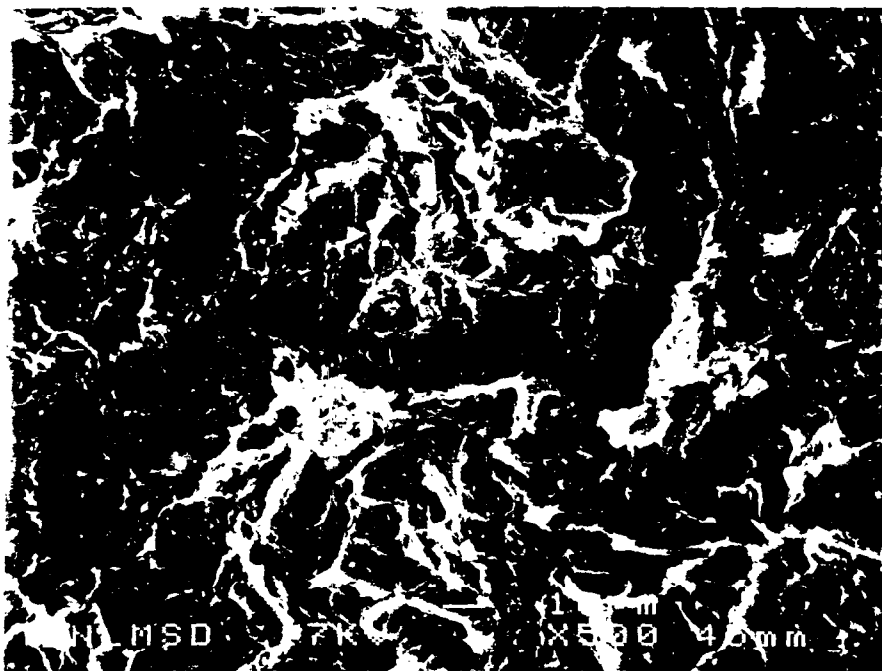


Figure 21. Polymer fracture surface showing tearing and coalescence of voids.

products themselves. Figures 19-21 depict the fracture surface of the polymer. Figure 19 shows pores in the polymer surface. Ductile tearing of the polymer around the edges of a pore is evident in Figure 20 (1-5B). Tearing is visible in Figure 21 (1-5A), as is coalescence of voids < 5 μm in diameter.

The ETFE coatings exposed to *T. ferrooxidans* exhibited biofouling in the liquid zone and surface staining from iron salts for above the liquid level. The coating material itself was not degraded by the bacteria. One of the panels displayed a blister 10 mm in diameter in the liquid zone. The coatings were removed with a razor blade to examine the steel condition. This method resulted in adhesive failure. It was found that spots of black corrosion products had formed at the interface between the steel and coating in both the liquid and vapour zones. Corrosion was more extensive in the upper half of the liquid zone than the lower. The least amount of corrosion was observed in a 5 mm band above the liquid level. This may be due to surface sealing by precipitated salts that act as an additional protective barrier.

Biofouling and surface staining were also observed for the EMAA coatings exposed to *T. ferrooxidans* and the polymer was not visibly attacked. The surface films were more adherent than for the ETFE coatings and could only be removed from the upper half of the liquid zone by scrubbing. Peel tests were performed and it was found that extensive surface corrosion had occurred beneath the coating. As was the case for the panels tested in brine, corrosion was manifested as black spots. The extent of corrosion was greater than that for the brine tests and was evident in both the liquid and vapour zones. The coatings used in the *T. ferrooxidans* tests were thinner, hence the results are not directly comparable. The distribution of the corrosion products differed for the bacteria tests. The individual spots of oxides increased in size with height of the liquid. The smaller spots of oxides corresponded with the greater extent of biofilm formation on the exposed surface of the coating. It is hypothesized that the biofilm tended to act as a sealant, thereby reducing penetration of aggressive species through the coating.

Directly above the liquid level was a band approximately 10 mm high that was completely devoid of visible corrosion. This apparently was a cathodic area and corresponded to tightly adherent iron salts on the external coating surface. Again, it is proposed that this surface layer acted as a sealant and actually improved the coating performance. The extent of corrosion on the steel substrates was similar for the EMAA and ETFE coatings.

Failure in these panels was totally adhesive. The peel load versus displacement curves showed similar form to those obtained from the panels exposed to brine. The strips cut from outside the test cell had relatively a constant load required to peel the coating. The average peel strength was 6.64 N/mm. Load versus displacement curves obtained from area of exposed coating had a bathtub shape with higher loads being measured outside the test cell. Plastic deformation of the EMAA also occurred in the latter areas. The extent of plastic yielding was greater than for the thicker coatings used in the brine tests due to higher bending

stresses. The peel strengths in the corroded areas were as low as 0.46 N/mm. Peel forces were less variable where corrosion occurred than for the specimens tested in brine and this is attributed to the absence of cohesive failure which is associated with higher loads and more extensive corrosion. Figure 22 is an example of peel test results in the exposed area. The spike in the flat section of the curve correlated with the uncorroded area directly above the liquid level.

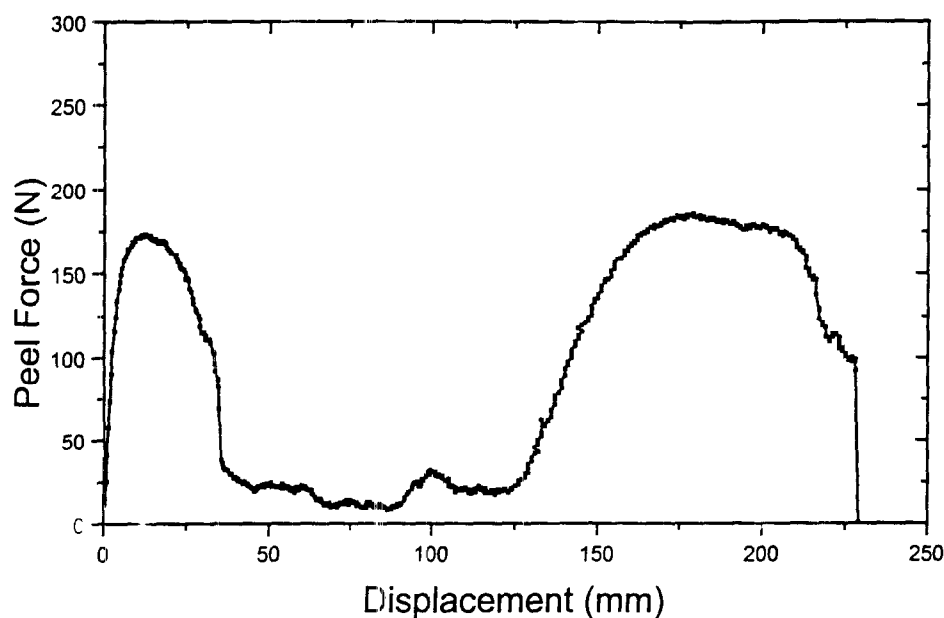


Figure 22. Peel force-displacement curve for EMAA exposed to *T. ferrooxidans*.

3.3 Cathodic Disbondment Tests

The rest potential of the unpolarized specimens after four weeks of exposure to brine ranged from -662 to -695 mV SCE. Pitting corrosion was evident at the coating holiday. Specimens polarized to potentials of -780 and -900 mV SCE did not undergo any cathodic disbondment. Slight corrosion occurred at the holidays indicating that a more negative potential is required for adequate cathodic protection under the conditions studied. No apparent disbondment and slight corrosion occurred at a potential of -1070 mV SCE. When the potential was decreased to -1500 mV SCE one specimen exhibited disbondment. The diameter of the disbondment was 4.06 mm, compared with the original holiday diameter of 3.2 mm.

3.4 Abrasion Tests

The thermal sprayed EMAA coating exhibited very slight wear at the conclusion of the stirred tank experiment. The percentage mass loss was 0.07%. The abrasion resistance of this coating could be increased by adding a ceramic filler to form a polymer-ceramic composite. The Devcon coated tank showed negligible wear and the mass remained constant. Therefore, this coating has good abrasion resistance and is a suitable candidate for pilot-scale tests to protect the reactor vessels from the abrasive effects of sludge.

4.0 DISCUSSION

The coupon tests confirmed that corrosion of bare 316L stainless steel could be expected in geothermal brine and sludges. This is in concurrence with many previous studies of corrosion in geothermal fluids at higher temperatures (e.g., 2-6). Higher corrosion rates would be predicted if the brine contains dissolved H_2S or CO_2 . Corrosion is also a potential problem for plant equipment exposed to the *T. ferrooxidans* biocatalyst and protective coatings are required. The EMAA coating was resistant to microbial degradation and protected the 316L from corrosion in the coupon tests. The baked PVDF and ETFE coatings also afforded corrosion protection.

The ETFE coated panels were subject to disbondment and corrosion at the interface between mild steel substrate and polymer when tested in brine with the Atlas cell arrangement. The low residual adhesion in the exposed area suggests that this coating will have insufficient long-term durability for protection of mild steel from brine. Performance of the ETFE coatings was better in the *T. ferrooxidans* environment. However, substrate corrosion tends to preclude the mild steel-ETFE system from the application of interest.

The Atlas cell tests for the EMAA coatings exposed to brine showed that corrosion at the interface was also a problem and that adhesion decreased where corrosion occurred. It was not clear why one of the panels tended to undergo corrosion primarily in the vapour zone, while the nominally identical companion panel corroded in both the liquid and vapour zones. The EMAA coatings cannot be recommended for long-term protection of mild steel from brine under the planned operating conditions. Future work will repeat the same tests on 316L substrates, since vessels of this material will be used in pilot scale biochemical processing of the geothermal residues. It is predicted that longevity of the 316L will be extended by EMAA coatings, although further testing is required to confirm this. The EMAA coatings did not adequately protect mild steel from corrosive effects of the *T. ferrooxidans* medium under the test conditions. The tests did reveal that sealing of the surface by deposits from the medium improved the barrier effect of the coating. Therefore, superior performance could be achieved if porosity of the coating can be reduced. Although corrosion of mild steel occurred with both the ETFE and EMAA coatings, it should not be neglected that the test environments were severe and that corrosion would have been rapid in the absence of the coatings.

The results from the initial cathodic disbondment tests in brine at room temperature indicate that the coating resists disbondment at potentials of -780 to -1070 mV SCE. However, corrosion of the mild steel substrate still occurred at these potentials. More negative potentials would increase the risk of disbondment. In addition, higher temperatures can be expected to increase the disbondment rate. These effects have been documented (7). Cathodic disbondment may also involve an initiation period (7). Hence, increased testing periods and elevated test temperatures are recommended before using the EMAA coatings in conjunction with cathodic protection at 55°C.

5.0 FUTURE WORK

Assuming funding is available, the evaluation of Devcon ceramic-filled epoxy coatings will continue. It is also planned to test coatings under pilot-scale operating conditions so that realistic working conditions, including temperature cycling and abrasive wear, are incorporated. Other coatings such as glass flake vinyl and polyesters also have potential. The combined effects of sulphur-oxidizing bacteria and geothermal residue will be examined. A new variation of the biochemical treatment involves a chemical reagent step. Therefore, it is necessary to determine the corrosiveness of this reagent and suitable protective coatings. Thermal sprayed EMAA coatings will be tested further for protecting 316L stainless steel. Also of interest is the use of thermal sprayed polymer-ceramic composites since these are expected to have improved abrasion resistance.

6.0 CONCLUSIONS

Thermal sprayed EMAA and ETFE polymers are resistant to attack by hypersaline brine, geothermal sludge and *T. ferrooxidans*. The coatings are not suitable for long-term protection of mild steel from these aggressive environments at 55°C due to corrosion and subsequent decrease in adhesion. EMAA has potential for protection 316L stainless steel and for use in conjunction with cathodic protection. Devcon Brushable Ceramic has excellent abrasion resistance. Although the long-term durability tests on this latter coating are not complete, initial indications are that it appears suitable for the application of interest and will be used in the pilot-scale tests. Spray-and-bake ETFE and PVDF coatings displayed good performance in coupon tests.

7.0 ACKNOWLEDGMENTS

The author is grateful to Professor C.C. Berndt, Dr. J.A. Brogan and Mr. D. Otterson (SUNY at Stony Brook) for preparation of thermal sprayed specimens and conducting the peel tests. Thanks are also due to Mr. Ray Zatorski (Zatorski Coating Co.) for preparing some of the coated specimens and to Mr. Jeff Yablon (BNL) for supplying the *T. ferrooxidans*.

8.0 REFERENCES

1. ASM Metals Handbook, Volume 13, Ninth Edition, Ohio, 1987.
2. W.R. Braithwaite, W.R. and K.A. Lichti, "Surface Corrosion of Metals in Geothermal Fluids at Broadlands, New Zealand," in ASTM STP 717, pp. 81-112, L.A. Casper and T.R. Pinchback, Eds., American Society for Testing and Materials, 1980
3. S.W. Borenstein, "Susceptibility of Stainless Steel Weldments to Microbiologically Influenced Corrosion," Materials Research Society Symposium Proceedings, Volume 294, pp. 353-360, 1993.
4. S.W. Borenstein, Microbiologically Influenced Corrosion Handbook, Industrial Press Inc., New York, 1994.
5. J.P. Carter and F.X. McCawley, "In Situ Corrosion Tests in Salton Sea Geothermal Brine Environments," Journal of Metals, 30, pp. 11-15, 1978.
6. S.D. Cramer and J.P. Carter, "Corrosion in Geothermal Brines of the Salton Sea Known Geothermal Resource Area," in ASTM STP 717, pp. 113-141, L.A. Casper and T.R. Pinchback, Eds., American Society for Testing and Materials, 1980.
7. D.K. Heffner, "Fluoropolymer Linings in the Transportation Industry," Materials Performance, 31, No. 7, pp. 33-36, 1992.
8. B. Little, P. Wagner and F. Mansfield, "An Overview of Microbiologically Influenced Corrosion," Electrochimica Acta, 37, No. 12, pp. 2185-2194, 1992.
9. P.J. Loustannau and D. Horton, "EMAA Thermoplastic Powder Coatings in Shop and Field Applications," Materials Performance, 33, No. 7, pp. 32-36, 1994.
10. D.D. Macdonald, B.C. Syrett and S.S. Wing, "The Use of Potential-pH Diagrams for the Interpretation of Corrosion Phenomena in High Salinity Geothermal Brines," Corrosion, 35, No. 1, pp. 1-11, 1979.
11. P.B. Needham, S.D. Cramer, J.P. Carter and F.X. McCawley, "Corrosion Studies in High-Temperature, Hypersaline Geothermal Brines," Corrosion '79, Paper 59, NACE, 1979.
12. E.T. Premuzic, M.S. Lin, J-Z. Hin and K. Hamilton, "Geothermal Waste Treatment Biotechnology," in Proceedings of World Geothermal Congress, pp. 2769-2772, Florence, 1995.
13. L.R. Scharfstein, "Effects of Composition, Structure, and Heat Treatment on the

Corrosion Resistance of Stainless Steel," in Handbook of Stainless Steels, D. Peckner and I.M. Bernstein, McGraw-Hill, New York, 1977.

14. U. Steinsmo and J.I. Skar, "Factors Influencing the Rate of Cathodic Disbonding of Coatings," Corrosion, 50, No. 12, pp. 934-939, 1994.

15. B.C. Syrett, D.D. Macdonald and H. Shih, "Pitting Resistance of Engineering Materials in Geothermal Brines-I. Low Salinity Brine," Corrosion, 36, No. 3, pp. 130-139, 1980.